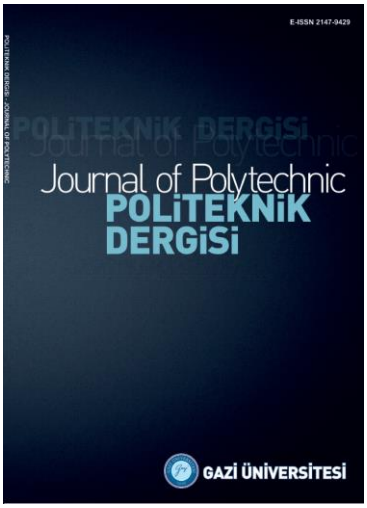

POLİTEKNİK DERGİSİ

JOURNAL of POLYTECHNIC

ISSN: 1302-0900 (PRINT), ISSN: 2147-9429 (ONLINE)
URL: http://dergipark.org.tr/politeknik

Dual band modified complementary split ring resonator loaded substrate integrated waveguide based bandpass filter

Çift bantlı değiştirilmiş tamamlayıcı ayrık halka rezonatör yüklü alttaş entegre dalga kılavuzu tabanlı bant geçiren filtre

***Yazar(lar) (Author(s))**: Galip Orkun ARICAN[1]*

ORCID[1]: 0000-0002-9375-886X

To cite to this article: Arıcan G. O., "Dual band modified complementary split ring resonator loaded substrate integrated waveguide based bandpass filter", ***Journal of Polytechnic***, 28(4): 1187-1193, (2025).

Bu makaleye şu şekilde atıfta bulunabilirsiniz: Arıcan G. O., "Dual band modified complementary split ring resonator loaded substrate integrated waveguide based bandpass filter", ***Politeknik Dergisi***, 28(4): 1187-1193, (2025).

Erişim linki (To link to this article): http://dergipark.org.tr/politeknik/archive

DOI: 10.2339/politeknik.1512729

Dual Band Modified Complementary Split Ring Resonator Loaded Substrate Integrated Waveguide Based Bandpass Filter

Highlights

- *The equivalent circuit of Dual-Band Microstrip bandpass filter is modelled*
- *A novel complementary split ring resonator (CSRR) with a bowtie shape is utilized in the design*
- *The EM simulations of the proposed design is performed with utilizing Finite Elements Method (FEM).*
- *S-parameters and group delay measurements are performed in the network analyzer.*

Graphical Abstract

In this study, a wideband DBPF is designed with single CSRR structure. Microstrip to SIW transition is implemented to further improve filter performance which is designed to be used in electronic warfare (EW) applications at H-, I- and J-bands. The simulation results are validated with the measurement results.

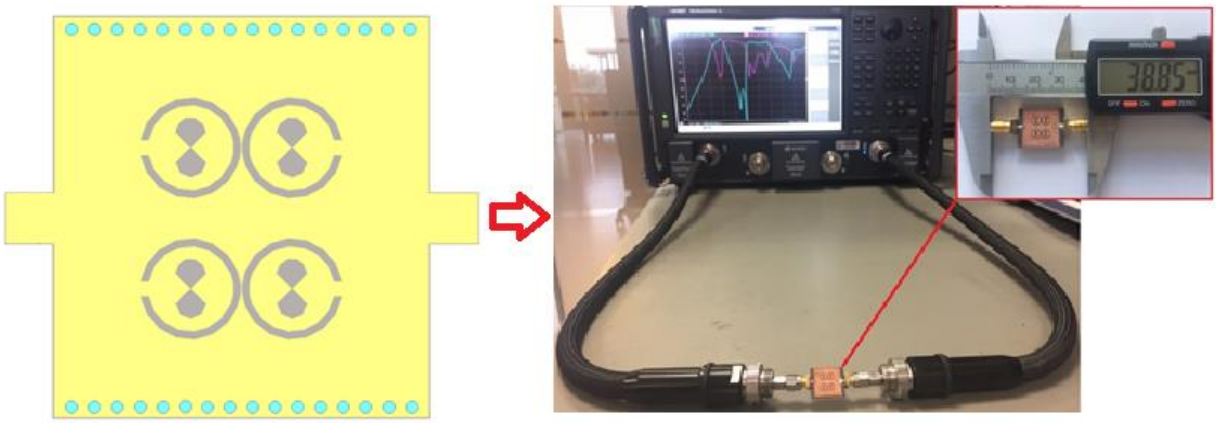

Figure. The layout and photography of the proposed BPF

Aim

In this study, it is aimed to develop a novel complementary split ring resonator loaded dual-band bandpass filter with utilizing substrate integrated waveguide (SIW) topology.

Design & Methodology

In the proposed design, an equivalent circuit is developed and the electromagnetic analysis is carried out with utilizing Finite Elements Method (FEM) and the validity of simulations are carried out with the measurements.

Originality

The proposed dual-band BPF with a novel complementary split ring resonator is a great candidate to be used for electronic warfare applications at H-, I- and J-bands.

Findings

The proposed design is validated with the measurements of the manufactured prototype. It is observed that the equivalent circuit model is coherent with both the layout simulation or measurements results.

Conclusion

In the measurements, it is observed that the center frequencies of the two passbands are around 6.6 and 12.6 GHz with the measured FBW values of 22.05% and 26.29%, respectively. The peak to peak group delay variation of the first passband (5.85-7.3 GHz) and second passband (10.9-14.2 GHz) are 108 ps and 676 ps, respectively.

Declaration of Ethical Standards

The author of this article declare that the materials and methods used in this study do not require ethical committee permission and/or legal-special permission.

Dual Band Modified Complementary Split Ring Resonator Loaded Substrate Integrated Waveguide Based Bandpass Filter

Research Article / Araştırma Makalesi

Galip Orkun ARICAN[1*]

[1]ASELSAN Inc., Communicaiton and Information Technologies Division, Ankara, Türkiye

(Geliş/Received : 08.07.2024 ; Kabul/Accepted : 17.12.2024 ; Erken Görünüm/Early View : 04.01.2025)

ABSTRACT

This study presents a dual-band bandpass filter design that implements microstrip to substrate integrated waveguide (SIW) transition to decrease radiation losses. The proposed filter is designed with using four complementary split ring resonators (CSRR) to minimize its size and to gain double negative property. A bowtie shaped slot is etched inside CSRR to have a second resonance at the spectrum. After the simulation results are performed the designed filter is fabricated on a Rogers RT5880 dielectric substrate and the experimental results are compared with the simulation results. The proposed filter has center frequencies at 6.57 and 12.55 GHz with fractional bandwidth (FBW) of 22.05% and 26.29%, respectively. Moreover, the presented filter offers the best bandwidth-to-size result with the size of $0.327\lambda_g \times 0.352\lambda_g$ (where λ_g is the wavelength at the first passband's center frequency).

Keywords: Substrate integrated waveguide (SIW), Microstrip filter, dual band, complementary split ring resonator (CSRR), bandpass filter.

Çift Bantlı Değiştirilmiş Tamamlayıcı Ayrık Halka Rezonatör Yüklü Alttaş Entegre Dalga Kılavuzu Tabanlı Bant Geçiren Filtre

ÖZ

Bu çalışma, ışıma kayıplarını azaltmak için alttaş entegre dalga kılavuzu (AED) geçişini mikroşeritten uygulayan çift bantlı bir bant geçiren filtre tasarımı sunmaktadır. Önerilen filtre, boyutunu en aza indirmek ve çift negatif özellik kazanmak için tamamlayıcı ayrık halka rezonatörü (TAHR) ile yüklenmiştir. İstenilen ikinci frekansta rezonansa sahip olmak için TAHR'ın içine papyon şeklinde bir yuva kazınmıştır. Benzetim sonuçları gerçekleştirildikten sonra, tasarlanan filtre Rogers RT5880 dielektrik alttaş üzerinde üretilmiş ve deneysel sonuçlar benzetim sonuçlarıyla karşılaştırılmıştır. Önerilen filtre, sırasıyla %22,05 ve %26,29 kesirli bant genişliği değerleri ile 6,57 ve 12,55 GHz'de merkez frekanslara sahiptir. Ayrıca sunulan filtre, $0{,}327\lambda_g \times 0{,}352\lambda_g$ (burada λ_g, ilk geçiş bandının merkez frekansında yönlendirilen dalga boyudur) boyutuyla en iyi bant genişliği-boyut sonucunu sunmaktadır.

Keywords: Mikroşerit filtre, çift bant, tamamlayıcı ayrık halka rezonatör (TAHR), alttaş entegre dalga kılavuzu (AED), bant geçiren filtre.

1. GİRİŞ (INTRODUCTION)

Metamaterial structures have been used frequently for the design of microwave elements in recent years in the form of split ring resonators (SRRs) [1-9] or as frequency selective surfaces (FSSs) [10-15]. An SRR structure, whether it is implemented to a filter, antenna or any kind of RF component, consists of a circular or rectangular shaped ring resonator with a gap at one edge. It is generally implemented on a dielectric substrate in the form of copper. These SRR structures can contain single, double or even triple rings. It is seen that as the number of nested resonators increases the bandwidth tends to increase as well [7]. Another way of using SRR is complementary SRR (CSRR), where the rings are etched from the plain copper. In [4], same SRR and CSRR structures are applied to the same filter design and it is seen that CSRR performs better results from the bandwidth and minimum rejection level point of view. Another important advantage of using SRRs and CSSRs in an RF component design is that they reduce circuit size as the designed resonators have dimensions much smaller in comparison to wavelength at the resonance frequency [16]. Meanwhile, when a dual-band characteristic is in need, a dual-band-pass filter (DBPFs) can be utilized to further decrease PCB size; as DBPFs will have a compact size in comparison to the cascade of two conventional bandpass filters. In the case of eliminating the unwanted band that high-power amplifiers and mixers will create, DBPFs [16-23] are employed to keep the two interested bands and reject a band in between them. Besides with accurate excitation of the SRR, negative permeability could be achieved while the excitation of the CSRR,

*Sorumlu Yazar (Corresponding Author)
e-posta : goarican@aselsan.com

negative permittivity could be achieved. Furthermore, features of achieving negative permeability and permittivity gathered with compact size makes adding SRR/CSRR structures convenient for high-performance filter design.

Substrate integrated waveguide (SIW) design is mostly implemented for microwave and mm-wave applications to prevent wave leakage due to very small wavelength [24-35], to reduce loss and to increase Q-factor for filter designs [36-38]. A broadband SIW bandpass filter is designed in [21] where a very high 3 dB fractional bandwidth (FBW) of 76% is achieved. Strongly electrically coupled CSRRs are implemented in [20] to create a DBPF with SIW transition.

In this study, a wideband DBPF is designed with single CSRR structure. Microstrip to SIW transition is implemented to further improve filter performance which is designed to be used in electronic warfare (EW) applications at H-, I- and J-bands. The validation of the proposed design is verified with the measurement results of the prototype. In addition, the center frequencies of DBPF are around 6.6 and 12.6 GHz with the measured FBW values of 22.05% and 26.29%, respectively. For the measured S-parameter results, the input reflection coefficient of the first passband is well below -10.3 dB in the frequency bandwidth of 5.85-7.3 GHz while second passband is below -10.5 dB in the frequency bandwidth of 10.9-14.2 GHz. The measured insertion loss of the first passband has a minimum value of -1.4 dB within the operating frequency bandwidth and the gain flatness is 0.7 dBpp. Moreover, the minimum S21 of the second passband is approximately around -2.8 dB in the 10.9-14.2 GHz frequency interval. The peak to peak group delay variation of the first passband (5.85-7.3 GHz) and second passband (10.9-14.2 GHz) are 108 ps and 676 ps, respectively. To the best of author's knowledge, this study is from one of the very few studies in which an SIW based dual bandpass filter is designed with CSRR structures. Furthermore, it has one of the most compact size with the dimensions of 14.9×16 mm^2; and its fabricated model provides great reflection coefficient, insertion loss and group delay results.

2. DESIGN OF SIW BASED DBPF

The designed SIW based DBPF is depicted in Fig. 1. Yellow color represents the copper material, grey represents the etched slots on the top of the filter, and cyan parts represent the plated through holes (vias). The input and output (I/O) ports are in the form of microstrip feeding line with a width of "a" (2 mm), which provides an impedance matching of 50 Ω. The proposed filter is designed on a RT5880 dielectric substrate. Additionally, in the design process, the relative permittivity (ε_r), dielectric loss tangent and dielectric thickness are taken respectively as 2.2, 0.0009 and 0.508 mm. The proposed design has a size of 14.9×16 mm^2, which corresponds to $0.327\lambda_g \times 0.352\lambda_g$ (where λ_g is the wavelength at the lowest center frequency). The bottom part is entirely plated with copper without any slits or slots. Copper thicknesses of the signal and ground planes are 0.035 mm. The side to side aligned via arrays prevent the undesired leakage by sort of creating a waveguide. Therefore, it is important to determine the diameter and spacing between vias; which are given as "d" and "s", respectively. Their values should be determined with respect to the operating frequency by using $\frac{d}{\lambda_g} \leq 0.1$ and $\frac{d}{s} \geq 0.5$ constraints [22]. The resonance frequency of the planar cavity resonator is dependent on SIW based DBPF geometrical dimensions with Eq. (1) [22].

$$f_{mn} = \frac{1}{2\sqrt{\varepsilon_r \mu_r}} \sqrt{\left(\frac{m}{L_{eff}}\right)^2 + \left(\frac{n}{W_{eff}}\right)^2} \quad (1)$$

$$W_{eff} = W_{SIW} - 1.08\frac{d^2}{s} + 0.1\frac{d^2}{W_{SIW}} \quad (2)$$

$$L_{eff} = L_{SIW} - 1.08\frac{d^2}{s} + 0.1\frac{d^2}{L_{SIW}} \quad (3)$$

where m and n represent TM, TE mode integers; ε_r, μ_r, W_{eff} and L_{eff} represent relative permittivity, permeability, effective width and length.

As seen in Fig. 1, single circular CSRR structure is preferred and a bowtie shaped slot is introduced inside the CSRR. A semi-circle is added to the edges of the bowtie to have a double band resonance at the desired frequencies. Moreover, the splits of the rings of the adjacent CSRRs are positioned back to back (both splits pointing outward) towards the input and output ports, this creates an electrical coupling characteristic [20]. It is seen that by positioning the outward looking CSRR couples attached to each other back to back, the coupling between the rings are further enhanced.

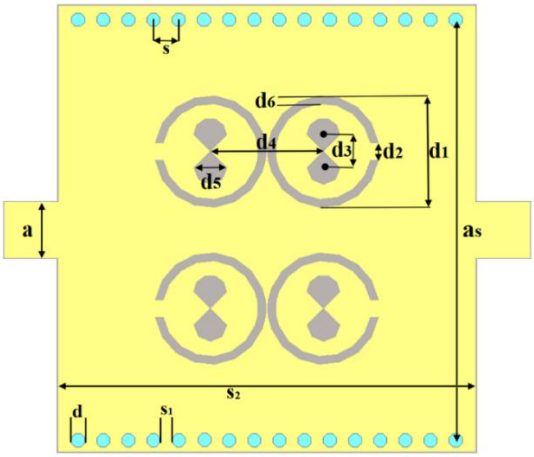

(*a*=2.0 mm, a_S=15.0 mm, *s*= 900 µm, s_1= 400 µm, s_2= 14.9 mm, *d*= 500 µm, d_1= 4.0 mm, d_2= 600 µm, d_3= 1180 µm, d_4= 4025 µm, d_5= 1200 µm, d_6= 300 µm)

Figure 1. Layout configuration of the proposed filter

The Keysight's commercially available PathWave EM Design (EMPro) software, which solves the EM problems with using Finite Element Method (FEM), is used for all the 3D EM analysis that are mentioned and

plotted in this study. Fig. 2 illustrates the reflection and transmission coefficients (S11 & S21) results of the designed DBPF. Simulation results are depicted as "EM Simulated". The simulated 3-dB FBW ($S_{21} \geq -3\ dB$) is calculated as 24.2% (5.8-7.4 GHz) for the first passband and 26.3% (11.05-14.4 GHz) for the second passband. It can be seen that dual-band characteristics are created and in between them there occurs a rejection band. In a conventional wave propagation scenario, it is accustomed that both permittivity (ε) and permeability (μ) of the medium/material is positive, which is also called as double positive. With a metamaterial design, more specifically with a CSRR design in our case, band rejection occurs since CSRR causes negative permeability in the vicinity of resonance frequency. It prevents the wave to propagate until permittivity becomes negative. This brings out the double negative ($\varepsilon < 0, \mu < 0$) property (left handed), where the wave propagation is allowed in the backward direction [25].

A parametric work is conducted to analyze the effects of the determined variables on S-parameters response. In Fig. 3(a), the effect of spacing between vias (s_1) is observed. It is seen that increasing the spacing between vias has a very little effect on the improvement of impedance matching in the second passband. However, the spacing between the via holes has a limit due to leakage of EM wave, as it is aforementioned. The variable d_3 again has a positive effect on S_{11} of second band. The best impedance matching is provided by 1180 µm, and it cannot be further scaled down due to manufacturing constraints. One of the most crucial parameter on filter performance is d_4, which is the distance between 2 adjacent CSRR couple. As seen from Fig. 3(c), the best result is obtained by positioning the rings attached to each other without giving any space, the reason of which was mentioned in the previous paragraph. By increasing the value of d_4 the second passband even disappears and the 50 Ω impedance matching of the first passband decays. In the last parametric study d_6 is changed, which is the thickness of the CSRR ring. It is seen that decreasing d_6 has a minor enhancement on filter performance. However, it can be further decreased from 300 µm due to fabrication constraints.

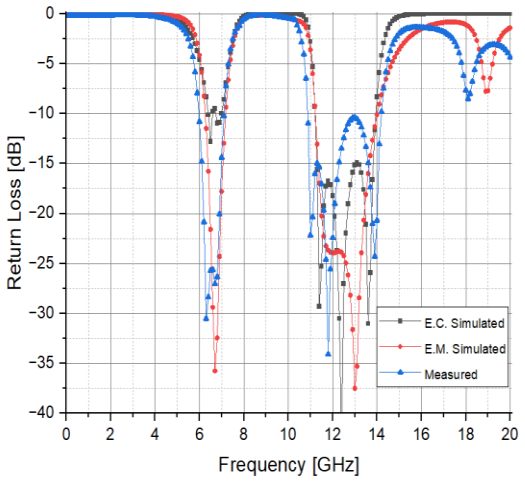

(a)

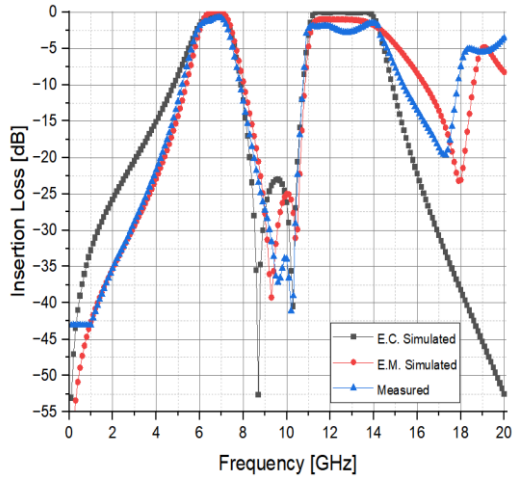

(b)

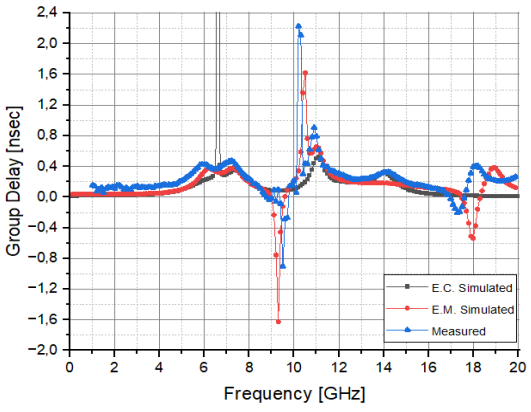

(c)

Figure 2. (a) Reflection coefficient, (b) insertion loss and (c) group delay simulation and measurement results.

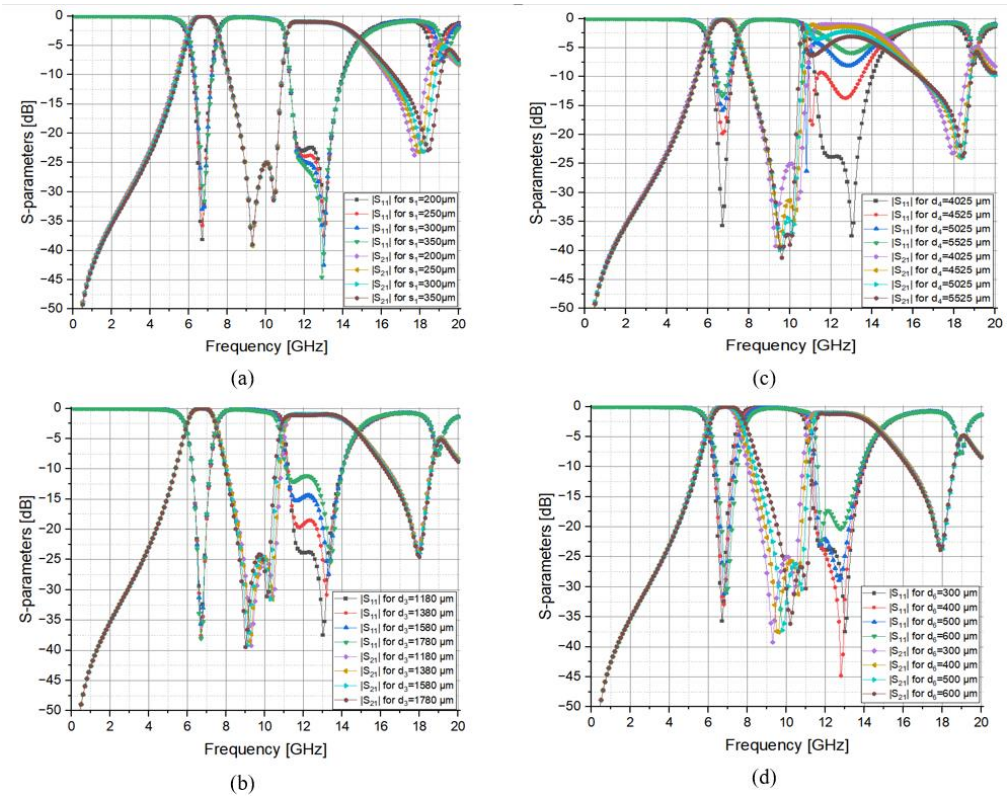

Figure 3. Parametric study for S-parameters according to variable (a) s_1, (b) d_3, (c) d_4, (d) d_6

3. FABRICATION AND EXPERIMENTAL MEASUREMENT OF SIW BASED DBPF

The proposed SIW based DBPF is fabricated and experimentally measured to verify its simulation results. One important point to note that it is important to maintain a fabrication quality above a certain level in SIW structures. Since a variation between the gap of the sidewalls might cause leakage. Therefore, the proposed filter is fabricated by utilizing LPKF Protolaser ST prototyping machine. Afterwards, the via holes are plated to achieve the electrical conductivity. Once the fabrication process is completed female SMA end launch connectors are soldered on both I/O ports of the filter. The S-parameters and group delay measurements are performed by utilizing Keysight N5224B network analyzer (10 MHz - 43.5 GHz) and Keysight N4651B electronic calibration kit to calibrate the network analyzer on the reference points as seen from Fig. 4(a). The center frequencies of the passbands are around 6.6 and 12.6 GHz with the measured FBW values of 22.05% and 26.29%, respectively.

For the measured S-parameter results, the S_{11} of the first passband is well below -10.3 dB in the frequency range from 5.85 to 7.3 GHz. Additionally, the S_{11} of the second passband is below -10.5 dB in the 10.9-14.2 GHz frequency interval. The measured S_{21} of the first passband has a minimum value of -1.4 dB within the operating frequency bandwidth as well as the gain flatness is 0.7 dB_{pp}. Moreover, the minimum S_{21} of the second passband is approximately around -2.8 dB in the 10.9-14.2 GHz frequency interval.

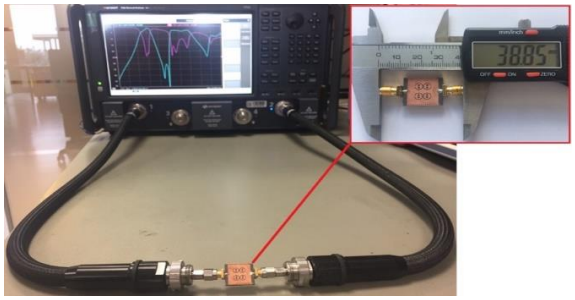

(a)

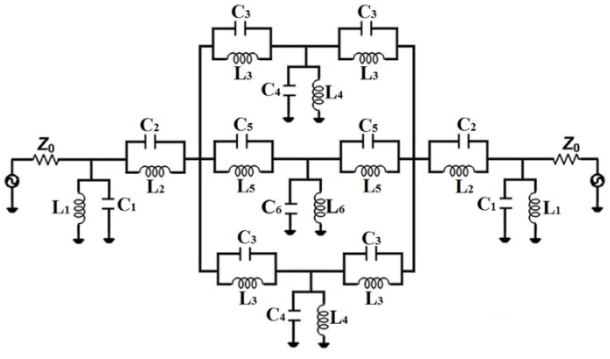

(b)

Figure 4. S-parameters measurement setup, (b) equivalent circuit model of the proposed DBPF design

The peak to peak group delay variation of the first passband (5.85-7.3 GHz) and second passband (10.9-14.2 GHz) are 108 ps and 676 ps, respectively.

CSRR structures can be modeled as L-C resonator tanks with a resonance frequency of $f_o = \left(2\pi\sqrt{LC}\right)^{-1}$ [7]. The equivalent circuit (EC) model is designed with lumped circuit elements to illustrate the effects of the CSRR and bowtie shaped slot etched CSRR and designed EC model is simulated in Keysight's ADS Schematic tool. As seen from Fig. 4(b), the EC model consists of parallel LC couples. The values of C_1, C_2, C_3, C_4, C_5 and C_6 are 695, 150, 1240, 1085, 570 and 470 fF, respectively. Moreover, the values of inductors L_1, L_2, L_3, L_4, L_5 and L_6 are 955, 290, 455, 570, 570 and 2245 pH, respectively. The return loss, insertion loss and group delay results of the EC model is given in Fig. 2. It is seen that the EC model provides proper results and good alignment is achieved with the measurement results.

Fig. 5 illustrates the electric field distribution over the proposed DBPF at 6.8 GHz (first passband), 9.6 GHz (stopband) and 12 GHz (second passband) frequency values. As seen from the figure, the electric field is distributed evenly and symmetrically between the I/O ports for both of the passband frequencies. As seen in Fig. 6(a), the filter operates at the dominant TE_{101} mode at 6.8 GHz and creates a resonance. The electric fields are mainly concentrated inside the CSRR rings and along the line between input and output terminals. At 9.6 GHz, which represents the stopband interval, the electric field fades away until it reaches the output terminal. This is the evanescent wave stage when the medium/material is converging from double positive to double negative property. For the second passband interval, in Fig. 6(c), again the electric field is evenly distributed between the I/O ports; the field is mainly concentrated between the two CSRR couples.

T here are few studies in literature where an SIW based DBPF is studied. Moreover, even in fewer paper, a CSRR or SRR structure is included in the design layout. The characterization of this work is checked with other state-of-arts in Table 1 to better verify its competitiveness. All the studies listed in the table are SIW based dual-band bandpass filters that include CSRR structures in their designs. The presented study offers the largest FBW for both bands along with the study in [20]. However, the proposed design has smaller size in λ_g when compared to [20].

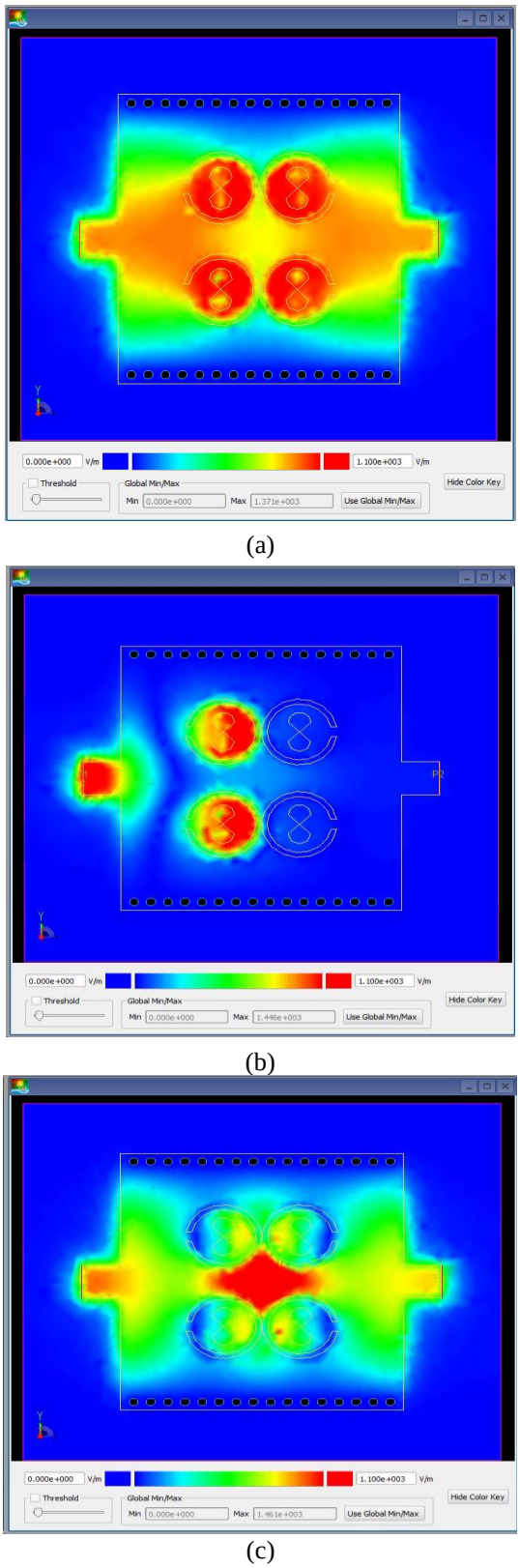

Figure 5. Electric field distribution (a) at 6.8 GHz (Passband1), (b) 9.6 GHz (Stopband) and (c) 12 GHz (Passband2)

Table 1. Comparison with other SIW based BPF studies

Ref.	# of Bands	CSRR Structure	f_{center} (GHz)	3-dB FBW (%)	IL (dB)	RL (dB)	Size ($\lambda_g \times \lambda_g$)
[5]	2	✓	7.9	3.4	1.5	14	0.87×0.85
			8.9	3.9	1.9	12	
[16]	2	✓	9.8	11.2	1.8	9.8	1.22×1.22
			13.5	9.8	1.5	10.6	
[17]	2	✓	1.94	14.43	1.26	15	0.179×0.097
			4.84	2.69	2.69	16	
[18]	2	✓	2.4	5.8	3.6	15	0.15×0.16
			5.2	6.5	3.1	15	
[19]	2	✓	3.2	14.2	0.9	31	0.24×0.12
			5.7	8	2.3	21	
[20]	2	✓	6.0	18.33	0.79	16.0	0.920×0.534
			12.0	29.17	1.39	9.0	
This work	2	✓	6.57	22.05	1.6	10.3	0.327×0.352
			12.55	26.29	2.8	10.5	

ACKNOWLEDGEMENT

The author is grateful to ASELSAN Inc. for providing the design tools and measurement infrastructure.

DECLARATION OF ETHICAL STANDARDS

The author of this article declare that the materials and methods used in this study do not require ethical committee permission and/or legal-spesific permission.

AUTHORS' CONTRIBUTIONS

Galip Orkun ARICAN: Carried out the design, production and measurement steps. Analyzed the experimental results and wrote the manuscript.

CONFLICT OF INTEREST

There is no conflict of interest in this study.

REFERENCES

[1] Choudhury A., & Maity S., "Design and fabrication of CSRR based tunable mechanically and electrically efficient band pass filter for K-band application", ***AEU-International Journal of Electronics and Communications***, 72: 134-148, (2017).

[2] Fu S-H. & Tong C-M., "A novel CSRR-based defected ground structure with dual-bandgap characteristics", ***Microwave Optical Technology Letters***, 51(12): 2908-2910, (2009).

[3] Khaled E.E.M., Saad A.A.R. & Salem D.A., "A proximity-fed annular slot antenna with different a band-notch manipulations for ultra-wide band applications", ***Progr Electromagn Res B***, 37: 289-306, (2012).

[4] Öznazı V., Ertürk V.B., "A comparative investigation of SRR- and CSRR-based band-reject filters: Simulations, experiments, and discussions", ***Microwave Optical Technology Letters***, 50(2): 519-523, (2008).

[5] Zhang H., Kang W. & Wu W., "Dual-band substrate integrated waveguide bandpass filter utilising complementary split-ring resonators", ***Electronics Letters,*** 57(2): 85-87, (2018).

[6] Bonache J., Gil I., Garcia-Garcia J. & Martin F., "Novel microstrip bandpass filters based on complementary split-ring resonators", ***IEEE Trans Microwave Theory Tech***., 54(1): 265-271, (2006).

[7] He X., Qiu L., Wang Y., Geng Z., Wang J. & Gui T., "A Compact Thin-Film Sensor Based on Nested Split-Ring-Resonator (SRR) Metamaterials for Microwave Applications", ***Journal of Infrared, Millimeter, and Terahertz Waves,*** 32(7): 902-913, (2011).

[8] Liu J., Lin H., Zeng B., Yeh K. & Chang D., "An Improved Equivalent Circuit Model for CSRR-Based Bandpass Filter Design With Even and Odd Modes", ***IEEE Microwwave and Wireless Components Letters***, 20(4): 93-195, (2010).

[9] Hu X., Zhang Q. & He S., "Dual-band-rejection filter based on split ring resonator (SRR) and complimentary SRR", ***Microwave Optical Technology Letters***, 51(10): 2519-2522, (2009).

[10] Ates S.H., Akcam N. & Okan T., "Bandwidth and Gain Enhancement using FSS on CPW-fed Rectangular Patch Antenna for 5G mm-Wave Applications", **International Congress on Human-Computer Interaction, Optimization and Robotic Applications (HORA)**, 09-11 June, (2022).

[11] Karahan M., Aksoy E., "Design and analysis of angular stable antipodal F-type frequency selective surface with multi-band characteristics. ***International Journal of RF and Microwave Computer-Aided Engineering***, 30(12): e22466, (2020).

[12] Can S., "Dual-band sub-6-GHz frequency filtering with optically transparent single-layer dual-polarized smart surface", ***Microwave and Optical Technology Letters***, 66(1): e33959, (2024).

[13] Doken B., Koç A. B., Koç İ. G. & Altan M., "Effectively Optimized Dual-band Frequency Selective Surface Design for GSM Shielding Applications", ***IETE Journal of Research***, 70(1), 199–205, (2022).

[14] Gürdal S., Aksimsek S. & Tokan N.T., "A triple-band frequency selective surfacefor 5G millimeter-wave communications", ***Microwave Optical Technology Letters***, 65: 2697-2703, (2023).

[15] Sondas A., "An FSSstructure with a band-stop performance for UWB applications", ***Microwave Optical Technology Letters***, 65: 480-485, (2023).

[16] Shi L-F, Sun C-Y., Chen S., Liu G-X. & Shi Y-F. Dual-band substrate integrated waveguide bandpass filter based on CSRRs and multimode resonator", ***International Journal of RF and Microwave Computure Aided Engineering***, 28(9): e21412, (2018).

[17] Yin B. & Lin Z., "A Novel Dual-Band Bandpass SIW Filter Loaded with Modified Dual-CSRRs and Z-Shaped Slot", ***AEU-International Journal of Electronics and Communications***, 121: 153261, (2020).

[18] Xu S., Ma K., Meng F. & Yeo K.S., "Novel Defected Ground Structure and Two-Side Loading Scheme for Miniaturized Dual-Band SIW Bandpass Filter Designs", ***IEEE Microwave and Wireless Componenets Letters***, 25(4): 217-219, (2015).

[19] Danaeian M., Moznebi A-R. & Afrooz K., "Super Compact Dual-Band Substrate Integrated Waveguide Filters and Filtering Power Dividers Based on Evanescent-Mode Technique", ***AEU-International Journal of Electronics and Communications,*** 125:153348, (2020).

[20] Fu W., Li Z., Liu P., Cheng J. & Qiu X., "Modeling and Analysis of Novel CSRRs-Loaded Dual-Band Bandpass SIW Filters", ***IEEE Transactions on Circuits and Systems II: Express Briefs***, 68(7): 2352-2356, (2021).

[21] Duraisamy T., Kamakshy S., Karthikeyan S.S., Barik R.K. & Cheng Q.S., "Compact Wideband SIW Based Bandpass Filter for X, Ku and K Band Applications", ***Radioengineering***, 30(2): 288-295, (2021).

[22] Dokmetas B. & Akcam N., "Uydu haberleşme sistemleri için 8025-8400 MHz düşük gürültülü kuvvetlendirici tasarımı", **Journal of *Polytechnic***, 27(4), 1643-11648, (2024).

[23] Oz I., "GEO satellite orbit determination using spaceborn onboard receiver", **Journal of *Polytechnic***, 27(1): 101-108, (2022).

[24] Okan T., "Design and analysis of a quad-band substrate-integrated-waveguide cavity backed slot antenna for 5G applications", ***International Journal of RF and Microwave Computer-Aided Engineering***, 30(7): e22236, (2020).

[25] Okan T. & Akçam N., "Wideband Low Cost FR4 Epoxy Based Antenna with H-shaped Slot for V-band Applications", ***International Journal of RF and Microwave Computer-Aided Engineering***, 31(2): e22348, (2021).

[26] Bhardwaj P., Deivalakshmi S. & Pandeeswari R., "Compact wideband substrate integrated waveguide bandpass filter for X/ Ku-band application", ***International Journal of RF and Microwave Computer-Aided Engineering***, 31(6): e22634, (2021).

[27] Vineetha K.V., Siva Kumar M., Madhav B.T.P., Usha Devi Y. & Das S., "Flexible and Conformal Metamaterial based Microwave Absorber for WLAN, Wi-MAX and ISM Band Applications" ***Materials Technology***, 37(8): 592-609, (2022).

[28] Ozkan R., Mert O., Yılmaz Y., Ramazan F. ve Duman M. "Attenuation of EM waves emitted from inset feed type microstrip rectangular patch antenna by wet snow", ***Journal of Polytechnic***, 27(2): 455-459, (2024).

[29] Chu P., Zhu P., Feng J., Guo L., Zhang L., Zhu F., ... & Wu K., "Substrate integrated waveguide filter with flexible mixed coupling", ***IEEE Transactions on Microwave Theory and Techniques***, 71(9): 4003-4011, (2023).

[30] Akgun O. & Tokan N. T., "H-plane SIW horn antenna with enhanced front-to-back ratio for 5G applications", Turkish Journal of Electrical Engineering and Computer Sciences, 31(2), 249-262, (2023).

[31] García R., Coves Á., Herraiz D., San-Blas Á. A. & Bozzi, M., "Low-Loss Periodically Air-Filled Substrate Integrated Waveguide (SIW) Band-Pass Filters", ***IEEE Access***, 12: 3617- 3628, (2024).

[32] Guvenli K., Yenikaya, S. & Secmen, M., "A Parallel Connected Hybrid Microstrip-Substrate Integrated Waveguide Bandstop Filter", ***Elektronika ir Elektrotechnika***, *29*(6), 26-32, (2023).

[33] Nasser M., Celik, A. R. & Helhel, S., "SIW-DGS bandpass filter design for C band satellite communications", ***Sādhanā***, *48*(2): 55, (2023).

[34] Jiao M. R., Zhu F., Chu P., Yu W. & Luo G. Q., "Compact hybrid bandpass filters using substrate-integrated waveguide and stripline resonators", ***IEEE Transactions on Microwave Theory and Techniques***, *72*(1): 391-400, (2023).

[35] Gorur A. K., Dogan, E. & Gorur A., "Single-wideband and dual-band bandpass filters based on compact quadruple-mode resonator", ***Journal of Electromagnetic Waves and Applications***, *38*(3): 327-344, (2024).

[36] Messaoudi E. M., Perez J. D. M. & Boria V. E., "Compact substrate integrated waveguide wideband bandpass filter with post-manufacturing tuning capabilities", ***IEEE Access***, *11:* 2327-2341, (2023).

[37] Lin G., Dong Y. & Luo X., "Miniaturized quarter-mode SIW filters loaded by dual-mode microstrip resonator with high selectivity and flexible response", ***IEEE Microwave and Wireless Components Letters***, *32*(6): 660-663, (2022).

[38] Qu L., Zhang Y., Jing H., Liu J. & Fan Y., "Compact filtering crossover design based on SIW quintuple-mode resonators", ***Microwave and Optical Technology Letters***, *64*(2): 218-222, (2022).